Short Communication

The Effect of Strain Reversal during High Pressure Torsion on the Evolution of Microstructure and Hardness in Al-2.5wt% Mg alloy

K. Chadha[a*], P.P. Bhattacharjee[b]

[a]Planetary and Space Science Centre, University of New Brunswick
Fredericton, New Brunswick E3B 5A3, Canada
[b]Department of Material Science and Metallurgy, Indian Institute of Technology, Hyderabad, Kandi, Telengana
*Corresponding Author: kchadha@unb,ca

Abstract

The present work aims to investigate the effect of strain reversal during High Pressure Torsion (HPT) on the evolution of microstructure and hardness properties of Aluminium-Magnesium (Al-2.5%Mg) alloy. For this purpose, Al-2.5%Mg alloy was subjected to monotonically (CW) and strain reversal (CW-CCW) deformation by High Pressure Torsion (HPT). The samples were subjected to a series of rotations in monotonically and strain reversal deformation with same equivalent strains of 1, 4, 12, 24 and 60 under an applied load of 6 GPa and with 1 rpm under quasi-constrained conditions. It was observed that Al-2.5%Mg when subjected to different routes, follows same trend in the evolution of the ultrafine structure, i.e. initial recrystallized microstructure with large grain size throughout the disk, at low strain level sub grains with prominent LAGBs network inside the grains and ultimately at the higher strains ultrafine microstructure throughout the disk characterized by equiaxed grains separated by HAGBs. The only exception to this was observed in case of Al-2.5%Mg during high strains at the centre regions where the fraction of HAGBs was found strikingly less as compared to its counterpart during strain reversal deformation. Hardness homogeneity was not observed for Al-2.5%Mg where the hardness at the centre regions was observed to be lesser than the edge regions with exceptionally less hardness at centre for strain reversal specimens at higher strains.

Keywords: High Pressure Torsion, Aluminium Magnesium alloy, strain reversal, microstructure, hardness.

1. Introduction

Development of high strength structural materials through grain size reduction as conceived in the Hall-Petch relation ($\sigma_Y = \sigma_0 + kd^{-1/2}$) [1] has been a major driving force in the fabrication of Ultrafine Grained (UFG with grain size <1μm) and Nanostructured (NS with grain size <100 μm) materials with a large fraction of high angle grain boundaries (HAGBs).

Severe Plastic Deformation (SPD) is the most well-known top down approach for fabrication UFG and NS materials. Fabrication of materials by SPD is usually done by imposing very high plastic strain, without concomitant changes in the dimensions of the work pieces. SPD techniques such as Equi Channel Angular Processing (ECAP) [2], Accumulative Roll Bonding (ARB) [3] and High Pressure Torsion (HPT) [4] can now successfully produce a wide variety of bulk Ultra Fined Grained and Nano structured materials.

Amongst various SPD processing technique HPT has gained significant attention due to fact that large plastic strain value can be easily achieved in this process. The equivalent strain value in HPT can be calculated by:

$$\varepsilon \approx \frac{1}{\sqrt{3}} \frac{r}{h} \varphi \qquad (1)$$

where, r = radius of the disc (mm), h = height if disc (mm), φ = angle of rotation (radians) and ε = equivalent strain value.

According to the equation the strain is directly proportional to the radius of the disc, which indicates that at the centre the strain is ideally zero, whereas the strain is highest at the edges of the disc. The development of microstructure and mechanical properties have been intensely investigated by various authors on many pure and commercially pure (CP) metals during monotonous deformation [4-11]. Addition of metals like Magnesium in pure Aluminium results in increase in the strength of alloy as Mg influences dislocation generation and work hardening [12, 13]. In addition to it, Al-Mg alloy has a lower propensity for dynamic recovery as compared to CP Aluminium. Studies have shown that the addition of Mg has a considerable amount of effect on mechanical properties and microstructure during HPT processing [14, 15].

The stain path change during HPT can be easily achieved by monotonous and reversal strain deformation through the combination of monotonous (CW) and subsequent strain

reverse rotation (CW-CCW) (Fig. 1). The strain path change in the HPT process is a continuous process and the sample remain in the equipment throughout the processing operation.

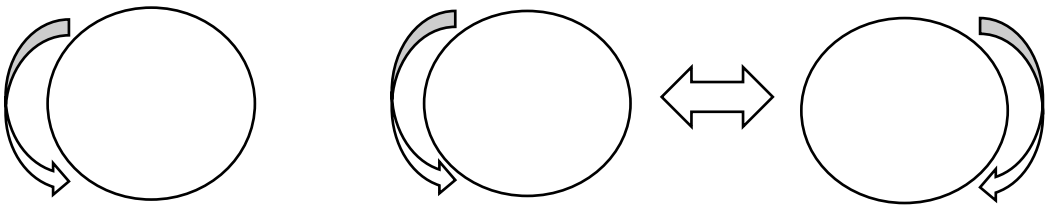

(a) (b)

Figure 1: Type of deformation, (a) Clockwise (b) Counter-Clockwise.

Strain reversal during HPT on the evolution of hardness and microstructure has been reported by a few researchers who have proved significant differences in microstructure and mechanical properties [5, 16]. It has been reported that disc subjected to strain reversal show limited increase in the hardness at the centre with increasing strain values, which is justified upon microstructure observation at the centre where grain refinement is limited [8]. A study on strain path change during cold rolling has shown differences in behaviour of microstructure and texture in Al and Al-Mg alloy [17]. There has been no studies focussing strain path change in HPT for Al-Mg alloys. The present study is determined to clarify these issues by studying microstructure and microhardness evolution during strain reversal of Aluminium-Magnesium (Al-2.5%Mg) alloy during HPT. It is envisaged that strain reversal would greatly affect the microstructure-property evolution in Al-2.5%Mg having lower propensity for dynamic recovery which essentially remains the main motivation for the present study.

2. Experimental

Al-2.5%Mg alloy was used for the present study. The as-received Al-2.5%Mg block (160mm (length) × 60mm (width) × 10mm (thickness)) was cold rolled to ~80% reduction in thickness and annealed in air furnace at 673K for one hour. The above material was used as the starting material for further processing. Disks with the diameter of 10mm were then cut from the sheet using EDM wire cut equipment. A total of 10 disks were cut for further HPT processing. These disks having 2 mm starting thickness were manually grinded to ~1.5mm thickness using SiC grit papers with grit size of 500, 1000 and 1200 respectively. The disks

were then designated according to the strain value or the number of rotations as per the given chart.

The disks were then deformed by HPT to the desired strain levels as shown in Table 1.

Table 1: Designation of the samples according to the strain

Monotonic	Strain Reversal	Equivalent Strain
CW 30_o	CW(15_o)-CCW(15_o)	1
CW120_o	CW(60_o)-CCW(60_o)	4
CW 1R	CW(180_o)-CCW(180_o)	12
CW 2R	CW(1R)-CCW(1R)	24
CW 5R	CW(2.5R)-CCW(2.5R)	60

CW- Clockwise Rotations, CW-CCW – Clockwise followed by counter clockwise

The imposed load was fixed at 390KN (~5GPa) and a rotation speed of 1 rpm was used at quasi-constrained conditions. The processing of the disks was done at POSTECH, South Korea in the group of Prof. H.S. Kim. To measure the hardness variation across the disk, Vickers microhardness test (Make: EMCO-TEST, Austria; Model: Dura Scan-70) was conducted on the disks. The disks were mounted using Hot Mounting Equipment (Make: Struss Citupress-10) and then manually grinded and polished in order to obtain a mirror finish. To measure hardness variation precisely, microhardness indentation points were taken 0.5mm apart from each other on two mutually perpendicular diameters of the disk under conditions of applied load of 200g with a dwell time of 15sec. The microstructure of the processed HPT disks was characterized by Electron Back Scattered Diffraction (EBSD) attached to a FEG-SEM (Make: Carl Zeiss; Model Supra 40) using Channel 5™ Software (Oxford Instruments, UK). EBSD measurements were taken on the r-ɵ plane of disks at the centre, middle and edge region of the disks. For EBSD investigations, the samples were polished mechanically using SiC paper of grit size 2000, followed by electropolishing using a mixture of perchloric acid and ethanol as electrolyte (1:9) at 20V and -30^0C (using Liquid N_2) for 20 sec.

3. Results

3.1 Microstructure Evolution

Fig. 2 shows the microstructure of the starting material. The grain size was measured 31µm with fraction of HAGBs around 68%. The microstructure reveals that the majority of the grains are recrystallized.

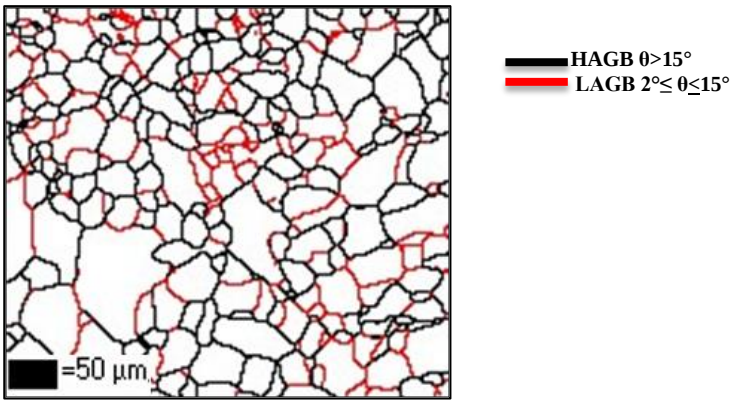

Figure 2: Microstructure graph of Al-2.5%Mg starting material.

The microstructural observations of the samples deformed by both deformation modes are shown in Fig. 3. Fig. 3 (a-e) shows microstructure of monotonous (CW) deformed specimens and Fig. 3 (f-j) shows microstructure of (CW-CCW) deformed specimens at ε=1,4,12,24,60 respectively. The variation in the average grain size and fraction of HAGBs w.r.t strain is plotted in Fig. 4 (a & b) for monotonically deformed specimens and strain reversal deformed specimens respectively. The high angle grain boundaries having misorientations $\theta \geq 15^{\circ}$ are marked in black and low angle boundaries with misorientations from 2° to 15° are marked in red.

Observation from Fig.3 (a-e) reveals that there is a continuous evolution of structure from LAGBs at lower strain to heterogeneous structure consisting of LAGBs and HAGBs at an intermediate strain level and ultimately resulting in an equiaxed ultrafine grained structure separated by mostly HAGBs. The microstructure evolution in case of strain reversal deformation (Fig. 3 (f-j)) is similar to the monotonous deformed specimens, where at starting LAGBs were found to dominate which then ultimately transforms to ultrafine grained structure at higher strains.

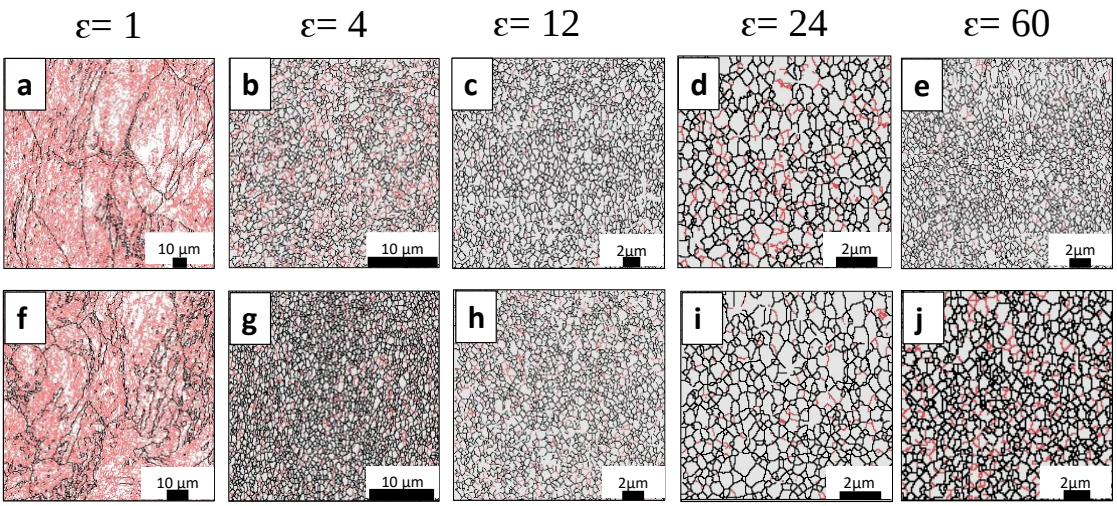

Figure 3: Grain boundary maps of Al-2.5%Mg, (a-e) monotonic deformed specimens and (f-j) strain reversal deformed specimens.

It can be inferred from Fig. 4 (a) that average grain size at the edge continuously decreases from ~8μm at ε=1 to 370nm at ε=60. The average grain size at ε=24 & 60 is nearly the same and thus signifying that grain size is saturated. The fraction of HAGBs (Fig. 4 (a)) also increases from 14% to 91% at ε=60. The fraction of HAGBs is observed nearly the same at strain levels ε= 12, 24 & 60.

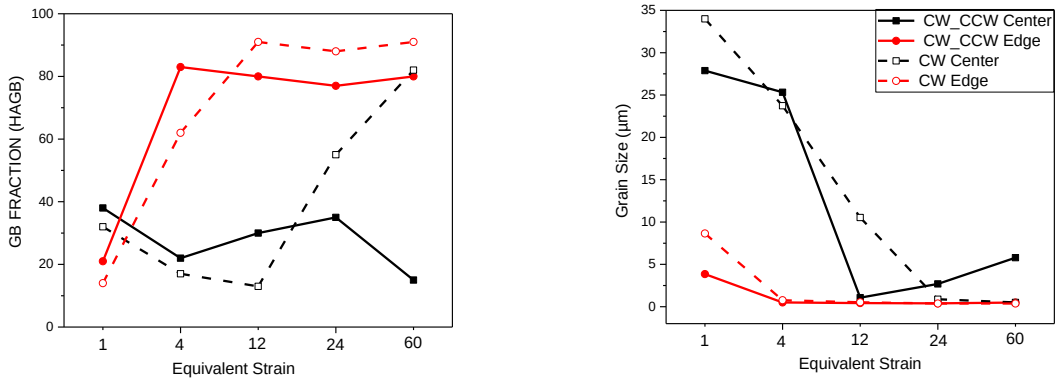

(a) (b)

Figure 4: Graph of grain size and Grain Boundary (GB) fraction versus equivalent strain for (a) monotonic deformation and (b) strain reversal deformation.

For strain reversal deformation, it can be observed from Fig. 4 (b) that average grain size at the edge continuously decreases from ε=1 to ε=60. However, the average grain size at the centre increases at ε=60, which is very surprising. Moreover, HAGBs fraction (Fig. 4(a)) increases from 21% at ε=1 to 82% at ε=4, thereafter no significant change is observed at the edge. It can be noted that the HAGBs fraction of strain reversal deformation at the edge region is less than the HAGBs fraction of monotonic deformation at nearly all strain levels.

3.2 Microhardness Evolution

The distribution of hardness values across the diameters is shown in Fig. 5 for the disks processed by HPT through monotonous (CW) and strain reversal (CW-CCW) deformation mode.

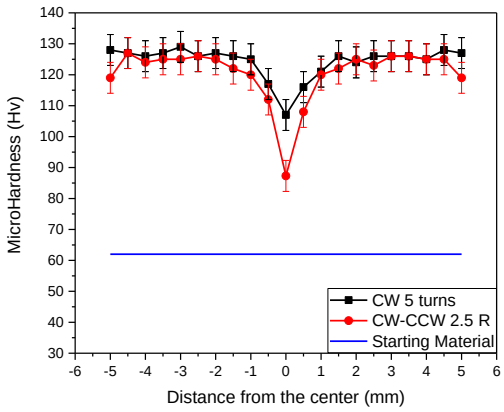

Figure 5: Hardness versus distance plot for monotonic and strain reversal deformed specimens

The characteristic hardness distribution of HPT processed disks with minimum in the centre and maximum at the edges can be easily seen at all strain levels. The hardness values of the monotonically and strain reversal deformed specimens at the same strain level are found to be very similar and shows very similar distribution characterized by higher hardness values at the edge and minimum at the centre which is typical for HPT processed disks. However, the major difference between the hardness distribution of the two processing routes is apparent at the highest strain level i.e. at ε=60. At this strain level the hardness at the edge regions (Fig. 6) of the monotonically and strain reversal deformed specimens are found to be very similar ~128 Hv and 125 Hv, respectively. On the other hand, at the centre region the hardness values are found to be different ~107 and 87, respectively, clearly indicating the

hardness at the centre of strain reversal deformed specimen is much lower than edges regions and also significantly lower compared to the centre regions of its monotonically deformed counterpart. It is clearly noted that hardness homogeneity is not achieved in any of the processing routes even after the imposition of such huge strain.

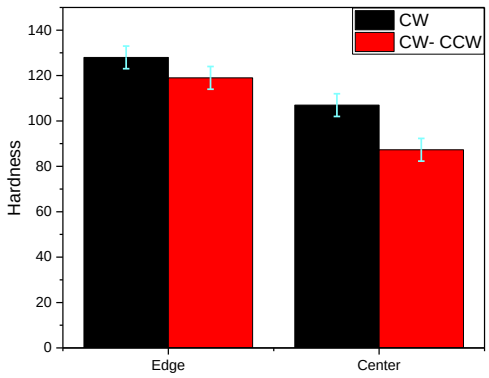

Figure 6: Comparison of the value of hardness at highest strain level (ε=60) at edge and centre deformed by monotonic (CW) and strain reversal (CW-CCW) deformation.

The evolution in the grain boundary fraction (Fig. 4 (a)) seems to be very interesting in this case. There is significant difference in the GB fraction after two different processing techniques. The monotonically (CW) deformed samples have higher amount of HAGBs as compared to the strain reversed (CW-CCW) deformed samples. The reason behind this could be Frank-Reed (F-R) Source of dislocation, in which is based on the dislocation multiplication in a slip place under shear stress [18]. During first clockwise rotation, the dislocations are generated and then during the proceeding counter-clockwise (strain reverse) rotation, another set of dislocation generated move in the opposite direction of the dislocations generated in the clockwise rotation. Due to this, there is a back stress and the dislocation sources are pinned down which during further rotations leads to less dislocation generation. Ultimately, due to less dislocation generation, at higher strains, there is less fraction of HAGBs in strain reversed (CW-CCW) deformation as compared to monotonous deformation (CW) deformation as schematically shown in Fig. 7.

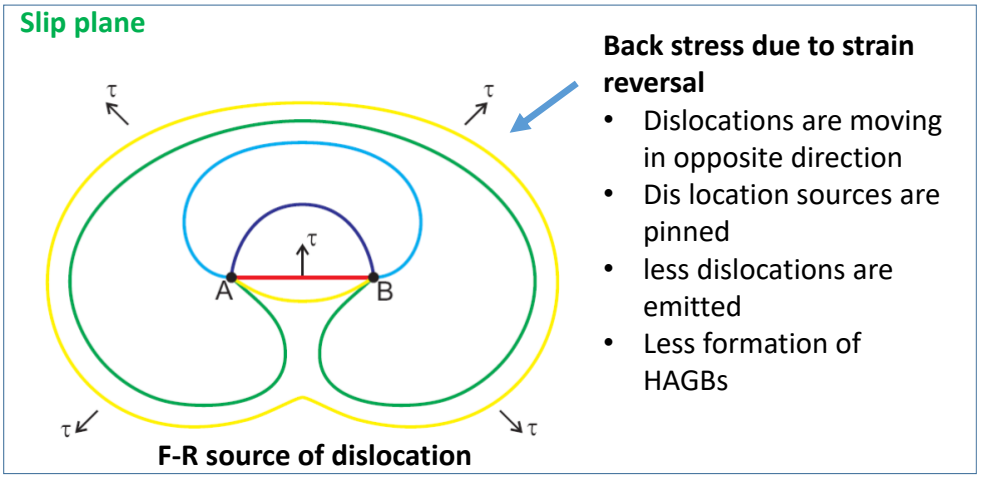

Figure 7: Schematic diagram showing back stress at dislocation source due to strain reversal deformation [18].

4. Conclusions

In the present work, an attempt was made to study the effect of strain reversal (CW-CCW) deformation on the microstructure and hardness properties of Al-2.5%Mg alloy. It was found that in Al-2.5%Mg, the evolution of the ultrafine structure follows the similar trend in microstructure analysis when deformed through two deformation techniques, with the exception during high strains where the fraction of HAGBs was found strikingly less as compared to its counterpart during strain reversal deformation. Hardness homogeneity was not observed for Al-2.5%Mg where the hardness at the centre regions was observed to be lesser than the edge regions with exceptionally less hardness at centre for strain reversal specimens at higher strains. The phenomenon behind low HAGBs in strain reversal deformation is predicted to be due to back stress due to strain reversal, which ultimately hinders the formation of dislocations formed by F-R source of dislocation

Acknowledgements

The authors are grateful to Prof. H.S Kim, POSTECH, Korea for processing the HPT specimens in his laboratory. The authors are also thankful to Department of Science and Technology (DST) for their financial support.

Conflict of Interest

The authors have no conflict of interest relevant to this article.

References

[1] Valiev RZ, Korznikov AV, Mulyukov RR. Structure and properties of ultrahne-grained materials produced by severe plastic deformation. 1993:141-.
[2] Valiev RZ, Islamgaliev RK. SPD processing and superplasticity in ultrafine-grained alloys. Superplasticity - Current Status and Future Potential Symposium, 29 Nov-1 Dec 1999. Warrendale, PA, USA: Mater. Res. Soc.; 2000. p. 335-45.
[3] Saito Y, Utsunomiya H, Tsuji N, Sakai T. Novel ultra-high straining process for bulk materials-development of the accumulative roll-bonding (ARB) process. Acta Materialia. 1999;47:579-83.
[4] Zhilyaev AP, Langdon TG. Using high-pressure torsion for metal processing: fundamentals and applications. Progress in Materials Science. 2008;53:893-979.
[5] Orlov D, Todaka Y, Umemoto M, Tsuji N. Role of strain reversal in grain refinement by severe plastic deformation. Materials Science & Engineering: A (Structural Materials: Properties, Microstructure and Processing). 2009;499:427-33.
[6] Orlov D, Todaka Y, Umemoto M, Tsuji N. Formation of bimodal grain structures in high purity Al by reversal high pressure torsion. Scripta Materialia. 2011;64:498-501.
[7] Kawasaki M, Figueiredo RB, Langdon TG. Twenty-five years of severe plastic deformation: recent developments in evaluating the degree of homogeneity through the thickness of disks processed by high-pressure torsion. Journal of Materials Science. 2012;47:7719-25.
[8] Zhang J, Gao N, Starink MJ. Microstructure development and hardening during high pressure torsion of commercially pure aluminium: Strain reversal experiments and a dislocation based model. Materials Science and Engineering: A. 2011;528:2581-91.
[9] Jiuwen Z, Nong G, Starink MJ. Microstructure development and hardening during high pressure torsion of commercially pure aluminium: Strain reversal experiments and a dislocation based model. Materials Science & Engineering: A (Structural Materials: Properties, Microstructure and Processing). 2011;528:2581-91.
[10] Xu C, Horita Z, Langdon TG. The evolution of homogeneity in an aluminum alloy processed using high-pressure torsion. Acta Materialia. 2008;56:5168-76.
[11] Kawasaki M, Alhajeri SN, Xu C, Langdon TG. The development of hardness homogeneity in pure aluminum and aluminum alloy disks processed by high-pressure torsion. Materials Science and Engineering A. 2011;529:345-51.
[12] Ryen Ø, Holmedal B, Nijs O, Nes E, Sjölander E, Ekström H-E. Strengthening mechanisms in solid solution aluminum alloys. MMTA. 2006;37:1999-2006.
[13] Hughes DA. Microstructural evolution in a non-cell forming metal: AlMg. Acta Metallurgica Et Materialia. 1993;41:1421-30.
[14] Zhang J, Gao N, Starink MJ. Al-Mg-Cu based alloys and pure Al processed by high pressure torsion: The influence of alloying additions on strengthening. Materials Science and Engineering A. 2010;527:3472-9.
[15] Gubicza J, Chinh NQ, Horita Z, Langdon TG. Effect of Mg addition on microstructure and mechanical properties of aluminum. Materials Science and Engineering A. 2004;387-389:55-9.
[16] Zhang J, Starink MJ, Gao N, Zhou W. Effect of Mg addition on strengthening of aluminium alloys subjected to different strain paths in high pressure torsion. Materials Science and Engineering: A. 2011;528:2093-9.
[17] Bhattacharjee PP, Saha S, Gatti JR. Effect of Change in Strain Path During Cold Rolling on the Evolution of Microstructure and Texture in Al and Al-2.5%Mg. J of Materi Eng and Perform. 2014;23:458-68.
[18] Frank FC, Mott NF. The Frank2014;Read source. Proceedings of the Royal Society of London A Mathematical and Physical Sciences. 1980;371:136-8.